

# Comparison between a proton, laser, and neutron test on Automotive MOSFETS for space application

A. Pesce<sup>1</sup>, M. Muschitiello<sup>1</sup>, F. Principato<sup>2</sup>, M. Ravituso<sup>3</sup>, C. Cazzaniga<sup>4</sup>, C. Frost<sup>4</sup>, M. Rizzo<sup>1</sup>, F. Pintacuda<sup>5</sup>

1) European Space Agency, Keplerlaan 1, 2200AG Noordwijk, The Netherlands  
[anastasia.pesce@esa.int](mailto:anastasia.pesce@esa.int), [michele.muschitiello@esa.int](mailto:michele.muschitiello@esa.int), [marta.rizzo@esa.int](mailto:marta.rizzo@esa.int)

2) Department of Physics and Chemistry, Palermo University, viale delle scienze, 90128 Palermo, Italy.  
[fabio.principato@unipa.it](mailto:fabio.principato@unipa.it)

3) HollandPTC, Huismansingel 4, 2629 JH Delft, The Netherlands  
[m.ravituso@hollandptc.nl](mailto:m.ravituso@hollandptc.nl)

4) ISIS Facility, STFC, Rutherford Appleton Laboratory, Didcot OX11 0QX, UK  
[carlo.cazzaniga@stfc.ac.uk](mailto:carlo.cazzaniga@stfc.ac.uk), [christopher.frost@stfc.ac.uk](mailto:christopher.frost@stfc.ac.uk)

5) STMicroelectronics, ADG-PTD, Stradale primosole 50, 95121, Catania (Italy),  
[francesco.pintacuda@st.com](mailto:francesco.pintacuda@st.com).

## Abstract

Proton and neutron irradiation tests on silicon and silicon carbide power MOSFETs for automotive applications were performed. Neutron tests are mandatory for the qualification of power devices for automotive applications. The aim of this work is to compare the neutron ruggedness of power MOSFETs with that of protons, required for power devices in low earth orbit (LEO) applications. The objective is to investigate if neutron characterizations, done for automotive power MOSFETs, could be used as pre-screening for Commercial-Off-The-Shelf (COTS) devices. Our investigations show a significant correlation between the sensitivity of power MOSFETs to protons and to neutrons. In addition, the use of a pulsed laser to simulate the interaction of protons and neutrons on the power devices is in progress.

## 1. Introduction

The current increase in the use of commercial nanosatellites (CubeSats) in the so-called New Space era, imposes the use of COTS devices. Indeed, the use of space-qualified components for these types of mission profiles is no longer attractive due to their high costs, long lead times, and lower performance [1,2]. Using COTS is a very challenging and sometimes risky business because the space environment is very harsh and has some conditions which were never taken into consideration while designing and manufacturing COTS semiconductor components [1].

Rad-Hard Power MOSFETs components qualified for space applications are characterized under proton and heavy-ion beams for different types of failures and degradations: Single Event Effect (SEE), Single Event Burnout (SEB), Single Event Gate Rupture (SEGR), Post Irradiation Gate Stress (PIGS), Total Ionizing Dose (TID). COTS components to be used in space missions have to be submitted to radiation-tolerance screening according to the space environment of the mission profile and associated Radiation Hardness Assurance (RHA) requirements. Useful standards for screening COTS devices are the ECCS-Q-ST-60-13 [3], ECSS-Q-ST-60-15[3], and NASA EEE-INST-002 [4].

Power MOSFETs used in automotive and avionic applications suffer from the impact of atmospheric neutrons generated from cosmic ray interactions with the atmosphere. The neutron interaction with power MOSFETs may cause SEB, which results in catastrophic device failure. Failure mechanisms in power semiconductor devices due to the cosmic radiation limit the maximum operating DC blocking voltage thus accelerated terrestrial neutron irradiations is

nowadays mandatory on commercial power MOSFETs for automotive applications to estimate their ruggedness to neutron interaction, even under atmospheric neutron flux at sea level altitude [5]. Accelerated neutron tests are usually performed according to the JEP151A procedure [6], by irradiating the power MOSFETs with high-energy neutrons (i.e. >10 MeV) at different drain-source bias voltages. The aim of these tests is to determine the failure rate in time (FIT, 1 FIT corresponding to on failure in  $10^9$  device-hours) values for the device at a given operating static condition.

The environment encountered by satellites in LEO is mainly characterized by the proton and electron particles trapped in the Van Allen belts. Power MOSFETs are susceptible to burnout when struck by a single proton. The aim of this work is to compare the neutron SEB susceptibility of power MOSFETs with that of protons. This comparison was performed by a focus on the range of drain voltages where the SEB events occur, without investigating the cross-section for both neutron and proton irradiations.

Moreover, for the same devices tested with neutron and proton beams, we are planning to perform destructive tests with a focused pulsed laser, to investigate the position dependence of SEB failure modes.

## 1. Test Vehicles

Table I shows the tested devices. These silicon and silicon carbide power MOSFETs are automotive devices, manufactured by STMicroelectronics and are available in the TO247 package. For the devices tested with the laser, the backside of the package was removed.

TABLE I.

LIST OF THE TESTED POWER DEVICES.

<i>Device</i>	<i>Part Number</i>	<i>Label</i>	<i>BV<sub>DSS</sub> (V)</i> & <i>Technology</i>
Si MOSFET	STH22N95K5	Si_A	950 V-Superjunction
Si MOSFET	SCB45N40DM2AG	Si_B	400 V-Superjunction
SiC MOSFET	SCT35N65G2VA	SiC_B	650-planar

### 2.1 Neutron Irradiation Test

The neutron irradiation was performed at the ChipIr beamline of the ISIS Neutron and Muon Source at the Rutherford Appleton Laboratory (Didcot, UK). The neutron beam has an atmospheric-like spectrum with a neutron flux  $\cong 5 \times 10^6$  cm<sup>-2</sup>s<sup>-1</sup> and energies up to 800 MeV. The selected collimated neutron beam size is 70×70 mm<sup>2</sup>. More information on the ChipIr was reported in [7]. The neutron tests were performed according to the JEP151A [6] procedure by using the Neutron Tester (made by STMicroelectronics and Department of Physics and Chemistry of Palermo University) which allow to control up to 24 devices per irradiation run, placed in three different boards, with the bias condition V<sub>gs</sub>=0 V and V<sub>ds</sub> at different values up to 1200 V.

### 2.2 Proton Irradiation Test

Proton irradiations were performed at the HollandPTC facility in Delft (Netherlands) [8]. The devices were irradiated at the R&D room of the Holland Proton Therapy Center facility which delivers monoenergetic proton beams in the energy range between 70 to 250 MeV. The R&D room is equipped with a beam monitor ionization chamber that monitor the incoming protons in real time. We used the pencil beam line characterized by a homogenous field in the whole area of the device. In the Figure 1 is shown a picture of the irradiation set-up. The test procedure used for proton irradiation is the same of that used in heavy-ion test, according to the ESCC-25100 test method. The devices were irradiated with a proton flux  $3 \times 10^8$  p/s cm<sup>2</sup> with 70, 100 and 200 MeV energies. For each irradiation run, the proton fluence was  $10^{11}$  p/cm<sup>2</sup>. At fixed energy the devices were irradiated at the following bias conditions: V<sub>gs</sub>=0 V, V<sub>ds</sub> in the range 250-650 V. Before and after irradiations, functional tests, the Sub-Threshold curves, the PIGS test and breakdown measurements were performed.



Figure 1. Proton irradiation set-up at the HollandPTC facility.

### 3.1 Results and discussions

Figure 2 shows the FIT values at sea-level of the test vehicles irradiated with neutrons as a function of the  $V_{ds}$  voltage and at  $V_{gs}=0$  V. The error bars indicate the 95% confidence interval. The FIT value of the Si\_A device at  $V_{ds}=600$  V, due to issues during the irradiation run, is an over-estimation of the true value. These curves highlight the threshold behaviour of the SEB failures as a function of the  $V_{ds}$  voltage.

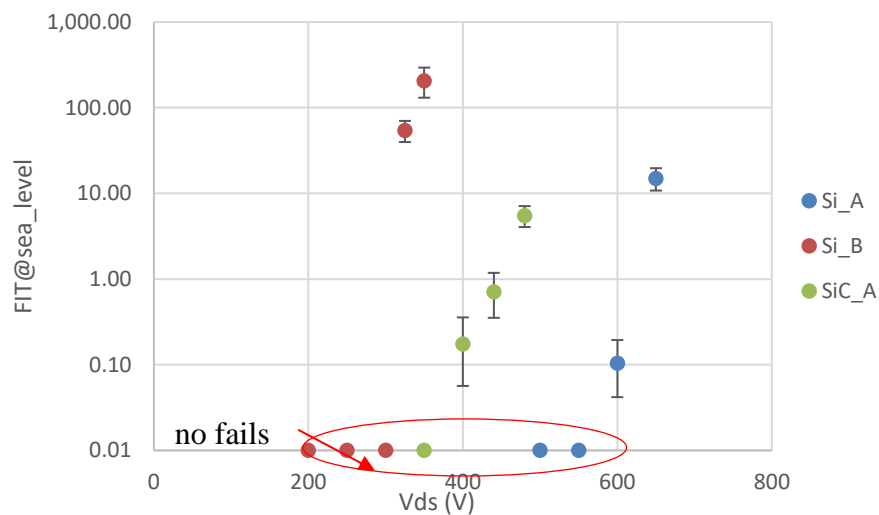


Figure 2. FIT at sea-level of the power MOSFET irradiated with neutrons at the Chip-Ir facility.

To compare the results of the neutron tests with those of protons, we consider for each irradiation run at fixed bias condition, the following quantities: in the case no fails occur during the run, we consider the neutron fluence  $\varphi_n$  for each device. When fails occur during irradiation, we consider the number of failed devices, the minimum, the maximum and the mean fluence for single device at the failure event ( $\varphi_{n, fail}$ ).

In the Tables I and II are shown the results of the neutron testes of the silicon devices Si\_A and Si\_B, respectively. The Table III are shown the data for the silicon carbide SiC\_A MOSFET.

TABLE I.  
Neutron test results of the silicon Si\_A power MOSFET

Vds (V)	Vgs (V)	$\varphi_n$ (n/cm <sup>2</sup> ·device)	Num. failed devices	Minimum $\varphi_{n,fail}$ (n/cm <sup>2</sup> ·device)	Mean $\varphi_{n,fail}$ (n/cm <sup>2</sup> ·device)	Maximum $\varphi_{n,fail}$ (n/cm <sup>2</sup> ·device)
500	0	$2.17 \times 10^{10}$	0	-	-	-
550	0	$1.20 \times 10^{10}$	0	-	-	-
600	0	-	7	*	*	*
650	0	-	19	$3.30 \times 10^7$	$6.10 \times 10^8$	$1.50 \times 10^9$

(\*): no data due to issues during the irradiation test.

TABLE II.  
Neutron test results of the silicon Si\_B power MOSFET

Vds (V)	Vgs (V)	$\varphi_n$ (n/cm <sup>2</sup> ·device)	Num. failed devices	Minimum $\varphi_{n,fail}$ (n/cm <sup>2</sup> ·device)	Mean $\varphi_{n,fail}$ (n/cm <sup>2</sup> ·device)	Maximum $\varphi_{n,fail}$ (n/cm <sup>2</sup> ·device)
200	0	$1.55 \times 10^{11}$	0	-	-	-
250	0	$1.40 \times 10^{10}$	0	-	-	-
300	0	$1.23 \times 10^{10}$	0	-	-	-
325	0	-	24	$5.83 \times 10^6$	$2.15 \times 10^8$	$1.00 \times 10^9$
350	0	-	24	$4.70 \times 10^7$	$5.40 \times 10^7$	$1.30 \times 10^8$

TABLE III.  
Neutron test results of the silicon carbide SiC\_A power MOSFET

Vds (V)	Vgs (V)	$\varphi_n$ (n/cm <sup>2</sup> ·device)	Num. failed devices	Minimum $\varphi_{n,fail}$ (n/cm <sup>2</sup> ·device)	Mean $\varphi_{n,fail}$ (n/cm <sup>2</sup> ·device)	Maximum $\varphi_{n,fail}$ (n/cm <sup>2</sup> ·device)
350	0	$1.42 \times 10^{11}$	0	-	-	-
400	0	-	5	$2.15 \times 10^7$	$1.93 \times 10^9$	$1.81 \times 10^{10}$
440	0	-	11	$6.64 \times 10^8$	$8.16 \times 10^9$	$9.82 \times 10^9$
480	0	-	17	$2.15 \times 10^7$	$1.93 \times 10^9$	$1.81 \times 10^{10}$

The data in Tables I, II, and III show the threshold drain voltages where the neutron SEB failure in power MOSFET occurs. These values are 600, 325, and 400 V for the Si\_A, Si\_B, and SiC\_A, respectively. We note that for irradiation runs performed at bias drain voltages lower than the threshold, the neutron fluence for each device without failures is orders of magnitude greater than the maximum neutron fluence at fail for irradiations made at drain voltage higher than the threshold value. For example, for the silicon Si\_B device at  $V_{ds}=300$  V, a neutron fluence up to  $1.23 \times 10^{10}$  ( $n/cm^2$ -device) does not cause SEB failures. At  $V_{ds}=325$  V it is sufficient a fluence of  $5.83 \times 10^6$  ( $n/cm^2$ -device) to induce catastrophic failures.

We observe that for the silicon carbide power MOSFET difference between the neutron fluences at  $V_{ds}$  lower the threshold and those above are less marked if compared with the data of silicon power MOSFETs. We suppose that in silicon carbide devices epitaxial defects can promote SEB mechanisms which make less marked respect to the silicon devices the threshold between the conditions where the SEB phenomenon triggers.

Tables IV, V, and VI show the results of the proton irradiations for the Si\_A, Si\_B, and SiC\_A power MOSFETs, respectively. For each irradiation run at a fixed bias condition, the Tables show the proton fluence  $\phi_p$  and energy, the occurrence of the SEB and SEGR events, and the results of the PIGS tests in the cases where neither SEB nor SEGR occurs.

TABLE IV.

Proton test results of the silicon Si\_A power MOSFET

$V_{ds}$ (V)	$V_{gs}$ (V)	$\phi_p$ ( $p/cm^2$ -device)	Proton energy (MeV)	SEB	SEGR	PIGS $V_{gs}$ (min,max)= $\pm 30$ V
550	0	$1.14 \times 10^{11}$	70	0	0	0
550	0	$1.05 \times 10^{11}$	200	0	0	0
600	0	$1.06 \times 10^{11}$	200	0	0	0
650	0	$4.85 \times 10^9$	200	1	-	-

TABLE V.

Proton test results of the silicon Si\_B power MOSFET

$V_{ds}$ (V)	$V_{gs}$ (V)	$\phi_p$ ( $p/cm^2$ -device)	Proton energy (MeV)	SEB	SEGR	PIGS $V_{gs}$ (min,max)= $\pm 30$ V
300	0	$9.10 \times 10^{10}$	200	0	0	0
300	0	$9.60 \times 10^{10}$	100	0	0	0
300	0	$1.07 \times 10^{11}$	70	0	0	0
325	0	$3.36 \times 10^{10}$	70	1	-	-
325	0	$9.78 \times 10^9$	200	1	-	-
250	0	$4.64 \times 10^{10}$	200	0	0	0

300	0	$1.87 \times 10^{11}$	200	0	0	0
350	0	$4.60 \times 10^9$	200	1	-	-

TABLE VI.

Proton test results of the silicon carbide SiC\_A power MOSFET

Vds (V)	Vgs (V)	$\phi_p$ (p/cm <sup>2</sup> ·device)	Proton energy (MeV)	SEB	SEGR	PIGS Vgs,min=-10 V Vgs,max=+22 V
350	0	$1.06 \times 10^{11}$	200	0	0	0
400	0	$1.10 \times 10^{10}$	200	1	-	-

We note that for both silicon and silicon carbide power MOSFET in the cases where no fails occur, the results of PIGS tests confirm that the gate oxide integrity is maintained after the proton irradiations. After proton irradiations, we performed electrical measurements on the survived power MOSFETs to investigate degradation effects due to the proton interaction with the sensitive volume of the power device.

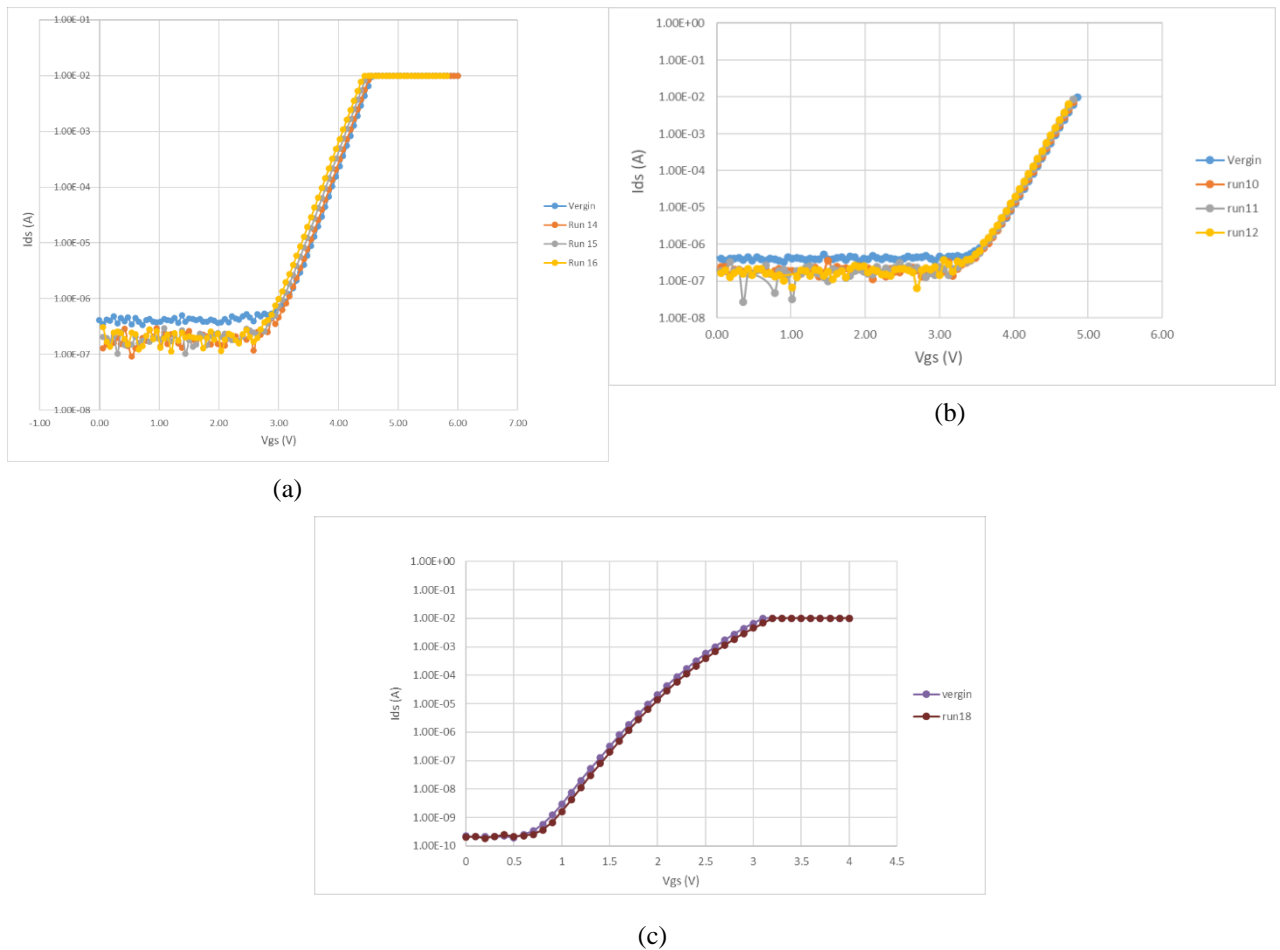
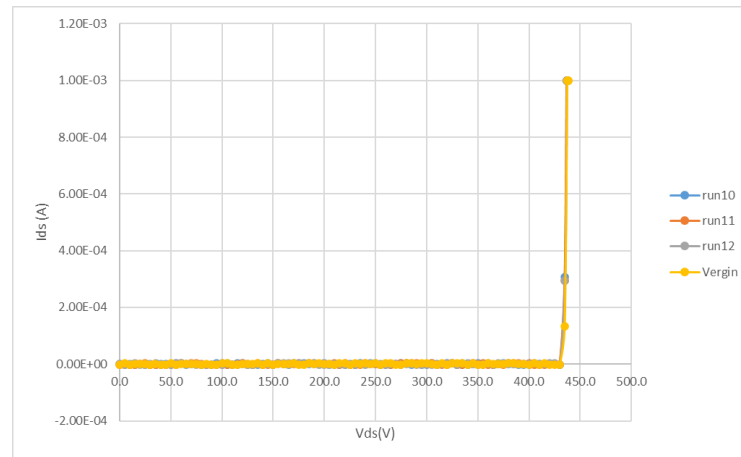
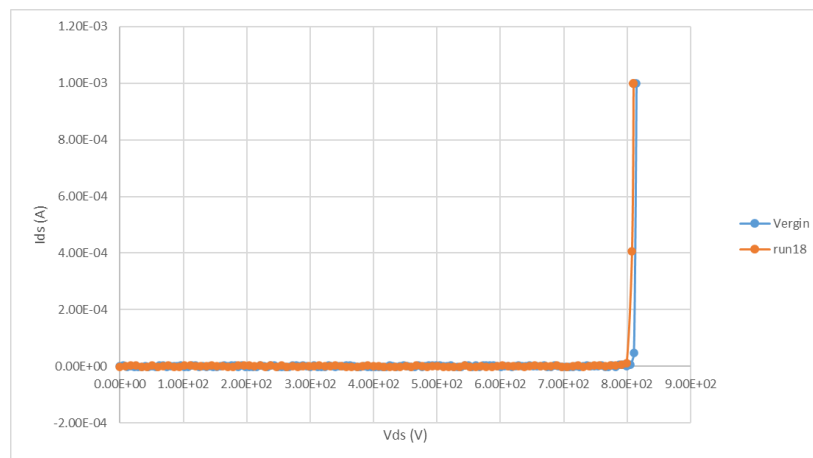


Figure 3. Sub-Threshold curves of the vergin and proton irradiated power MOSFETs, at different irradiation runs, with 200 MeV of proton energy. (a) Si\_A, (b) Si\_B and (c) SiC\_A.

In figure 3 are shown the sub-threshold curves for the vergin power MOSFETs and for the same devices after different irradiation runs with 200 MeV protons. We note a negative shift of the  $I_{ds}$ - $V_{gs}$  curves for both silicon devices, due to positive trapped charges in the gate oxide. The shift in the threshold  $V_{gs}$  voltage increases with the number of proton irradiation runs, that is the trapped charge in the gate oxide is proportional to the proton fluence. The threshold shifts, after the same proton fluence, in the Si\_A device is greater than those observed in the Si\_B device, due to the thicker gate oxide of the Si\_A with respect to the Si\_B one. In the whole power MOSFET we do not observe any change in the slope of the curves. This indicates that protons do not cause defects at the  $\text{SiO}_2/\text{Si}$  and  $\text{SiO}_2/\text{SiC}$  interfaces.



(a)



(b)

Figure 4. Breakdown curves of the vergin and proton irradiated Si\_B and SiC\_A power MOSFETs, at different irradiation runs, with 200 MeV of proton energy.

In figure 4 are shown the  $I_{ds}$ - $V_{ds}$  curves at  $V_{gs}=0$  V, for the reference (not irradiated) Si\_B and SiC\_A power MOSFETs and for the same devices after different irradiation runs with 200 MeV protons. We note no change in the avalanche voltage due to proton irradiations, regardless of the proton fluence. The same behavior is observed in the silicon Si\_A power MOSFET.

### 3.2 Comparison between proton and neutron irradiations

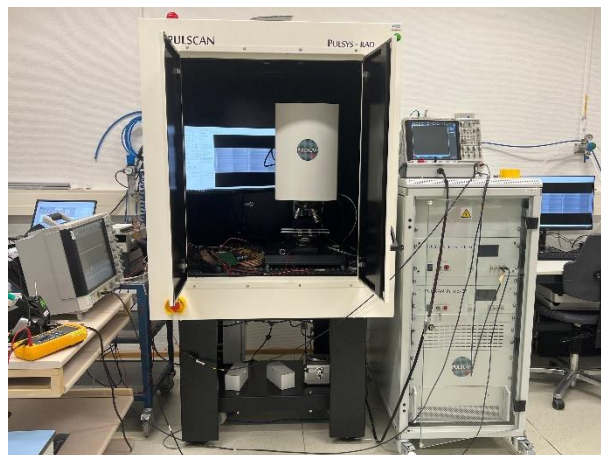
From the analysis of the data in Tables I-VI, we observe that in both proton and neutron irradiations only SEB failures occur. No SEGR failures during neutron irradiation were observed in previous experiments [5] for the same power devices. Concerning the proton irradiations, we note the lack of degradation for the power MOSFET which survived the test, except for the drift in the  $V_{gs}$  voltage threshold. The absence of any degradation due to neutrons for the power device which survived the neutron tests was observed in [9].

We note that the values of the threshold  $V_{ds}$  voltage over which SEB failure occurs during the proton irradiations are close to those observed in neutron irradiations for all test vehicles. For example, for Si\_B power MOSFET, the SEB threshold  $V_{ds}$  value is 325 V for both proton and neutron particles. These threshold values in the case of proton irradiations do not depend on the energy of the proton beam in the 70-200 MeV range.

The energy dependence on the neutron beam can not be investigated by using the white neutron beam with energies ranging between 10 and 800 MeV of the Chip-Ir facility. We note that the results of proton irradiation need further investigations to have more extensive statistics and negative  $V_{gs}$  bias conditions.

### 4. Laser Tests are ongoing

SEE Laser testing is foreseen for the future as a further development for this research. Tests are planned and ongoing both with SPA (Single Photon Absorption) and TPA (Two Photon Absorption) laser technologies. The aim is to simulate the interaction of high-energy particles with the device, so to gather relevant information for characterizing the power device. In this respect, laser tests allow obtaining spatial and temporal information on the occurrence of SEEs, which is useful to have for radiation hardening purposes.



. Figure 5. Laser test setup at the ESA-ESTEC facility.

A preliminary setup validation has been performed, and the collection of laser-generated charge has been seen on an the unbiased device Si\_B. The transient current induced by the pulsed infrared pulsed laser were read out through a CIVADEC 20dB current amplifier and a Keysight InfiniVision DSOX4154A oscilloscope.

### 4. Conclusions

In this work, we compare the results of irradiations with 70-200 MeV protons of silicon and silicon carbide power MOSFETs with those obtained with atmospheric-like neutron beams. The main result is that the threshold  $V_{ds}$  voltage over which the SEB failure in the power MOSFETs occur is the same for both proton and neutron irradiations.

In the case of proton irradiations, we note that the threshold  $V_{ds}$  voltage of the SEB failure does not depend on the energy of the proton beam in the 70-200 MeV range. The only difference between neutron and proton irradiation is that in the case of protons a trapped charge in the gate oxide occur in the power MOSFET which survive the irradiations. For these devices no degradation phenomena were observed in both proton and neutron irradiations.



Further investigations are in progress of proton irradiations to improve statistics and to investigate the negative Vgs bias conditions.

## References

- [1] H. Bokil, "COTS Semiconductor Components for the New Space Industry," *2020 4th IEEE Electron Devices Technology & Manufacturing Conference (EDTM)*, 2020, pp. 1-4.
- [2] Budroweit, J.; Patscheider, H. Risk Assessment for the Use of COTS Devices in Space Systems under Consideration of Radiation Effects. *Electronics* **2021**, *10*, 1008.
- [3] <https://ecss.nl>
- [4] "Instructions for EEE parts selection, screening, qualification and derating", EEE-INST-002, NASA Goddard Space Flight Center, 2003.
- [5] Principato F, Altieri S, Abbene L, Pintacuda F. Accelerated Tests on Si and SiC Power Transistors with Thermal, Fast and Ultra-Fast Neutrons. *Sensors*. 2020; 20(11):3021.
- [6] Test Procedure for the Measurement of Terrestrial Cosmic Ray Induced Destructive Effects in Power Semiconductor Devices. JEDEC Stand. 2015, JEP151.
- [7] Cazzaniga, C.; Frost, C.D. Progress of the Scientific Commissioning of a fast neutron beamline for Chip Irradiation. *J. Phys. Conf. Ser.* **2018**, *1021*, 012037.
- [8] M. Rovituso, A. Constantino, T. Borrel, W. van Burik, E. Schenk, A. Pesce, "The HollandPTC R&D proton beam line for radiation hardness tests in space application", submitted to RADECS 2022 conference.
- [9] Principato F, Allegra G, Cappello C, Crepel O, Nicosia N, D'Arrigo S, Cantarella V, Di Mauro A, Abbene L, Mirabello M, Pintacuda F. Investigation of the Impact of Neutron Irradiation on SiC Power MOSFETs Lifetime by Reliability Tests. *Sensors*. 2021; 21(16):5627.